

Casein Micelles: Size Distribution in Milks from Individual Cows

C. G. (Kees) de Kruif^{*,†,§} and Thom Huppertz[†][†]NIZO food research, P.O. Box 20, 6710 BA Ede, The Netherlands[§]Van 't Hoff Laboratory for Physical and Colloid Chemistry, Utrecht University, Padualaan 8, 3584 CH Utrecht, The Netherlands

ABSTRACT: The size distribution and protein composition of casein micelles in the milk of Holstein-Friesian cows was determined as a function of stage and number of lactations. Protein composition did not vary significantly between the milks of different cows or as a function of lactation stage. Differences in the size and polydispersity of the casein micelles were observed between the milks of different cows, but not as a function of stage of milking or stage of lactation and not even over successive lactations periods. Modal radii varied from 55 to 70 nm, whereas hydrodynamic radii at a scattering angle of 73° ($Q^2 = 350 \mu\text{m}^{-2}$) varied from 77 to 115 nm and polydispersity varied from 0.27 to 0.41, in a log-normal distribution. Casein micelle size in the milks of individual cows was not correlated with age, milk production, or lactation stage of the cows or fat or protein content of the milk.

KEYWORDS: casein micelles, composition, density and size distribution

■ INTRODUCTION

Casein micelles in milk are the delivery vehicle to, the neonate for high levels of calcium and phosphate, required for its bone growth. Approximately 70% of bone and ~90% of tooth enamel of the rapidly growing neonate consists of calcium phosphate, which is in the hydroxyapatite form ($\text{Ca}_5(\text{PO}_4)_3\text{OH}$). For bone and tooth mineralization, the neonate depends solely on calcium and phosphate from milk; for bovine milk the levels are ~30 mmol L^{-1} calcium and ~20 mmol L^{-1} inorganic phosphate.¹ Like most other calcium phosphates, hydroxyapatite is only sparingly soluble in water, having a solubility product of 2.34×10^{-59} , which corresponds to a solubility of ~0.4 mmol L^{-1} . Even though the solubility of calcium phosphates is slightly higher in milk serum than in water,^{2,3} this concentration is still far too low to sustain the demands of the neonate. To solve this problem, and prevent pathological calcification of the mammary gland, the transport of calcium phosphate in milk is in an encapsulated yet bioavailable form, that is, casein micelles.⁴

Many reviews^{5–18} have been devoted to the casein micelle. The general picture is that of a proteinaceous particle with a typical (volume-average) radius of ~100 nm.¹² Casein micelles contain ~3.4 g of H_2O per gram dry matter,¹⁹ and the dry matter consists of ~93% protein and ~7% inorganic material, collectively referred to as micellar calcium phosphate (MCP).¹² Although the exact substructure of the micelles is still a topic of debate,^{7–10,12,15–18} which is outside the scope of this study, there is now consensus that MCP is present in the form of so-called nanoclusters.^{9,12,17} Due to supersaturation of calcium phosphate in the mammary gland,⁴ nanometer-sized clusters of amorphous calcium phosphate are formed, the growth of which is stopped by absorption of the centers of phosphorylation of α_{s1} -, α_{s2} -, and β -casein onto the surface of the calcium phosphate nanoclusters. These thermodynamically stable nanoclusters have a radius of ~9 nm and consist of a core (~2 nm) of amorphous calcium phosphate and a shell of caseins.^{17,20,21} The more hydrophobic parts of the casein protrude from the surface of the nanoclusters and self-associate

into larger structures.^{12,17} The association process is terminated when the surface of the particle becomes hydrophilic, through the adsorption of κ -casein and β -casein, which have hydrophilic C-termini that protrude into the surrounding solvent, stabilizing casein micelles as a polyelectrolyte brush.²²

Although there is reasonable agreement on the biochemistry of the caseins and the composition of the casein micelles, reported numbers and values for various physical properties of casein micelles show extremely wide variation. In some cases, the numbers given are not even self-consistent; that is, there must be a one-to-one relationship between casein concentration, voluminosity, number of casein micelles, particle radius, and volume fraction of casein micelles in milk, but this is not always apparent from data reported in the literature. One source of confusion is certainly in the use of dynamic light scattering (DLS) for particle size measurements, wherein results depend on the used (manufacturers) algorithms, the spacing of the correlation time, the scattering angle, and the preparation and polydispersity of the sample, as will be shown below. It was for this reason that we decided to re-evaluate some of the characteristics of casein micelles with the aim of providing a uniform and self-consistent picture. Therefore, we investigated the variability in casein micelles size and composition within a herd of Holstein-Friesian cows as a function of stage of milking and stage of lactation and over several lactations. Our results are discussed and the interpretation and differences in the numbers presented.

■ MATERIALS AND METHODS

From a herd of 120 Holstein-Friesian cows, a total of 18 cows were selected to provide a wide variation in stage of lactation (from 4 to 28 weeks postpartum at first sampling), number of lactations (1–9), age of the cow (2–10 years of age), and milk production figures. The first

Received: April 3, 2012

Revised: April 6, 2012

Accepted: April 9, 2012

Published: April 9, 2012

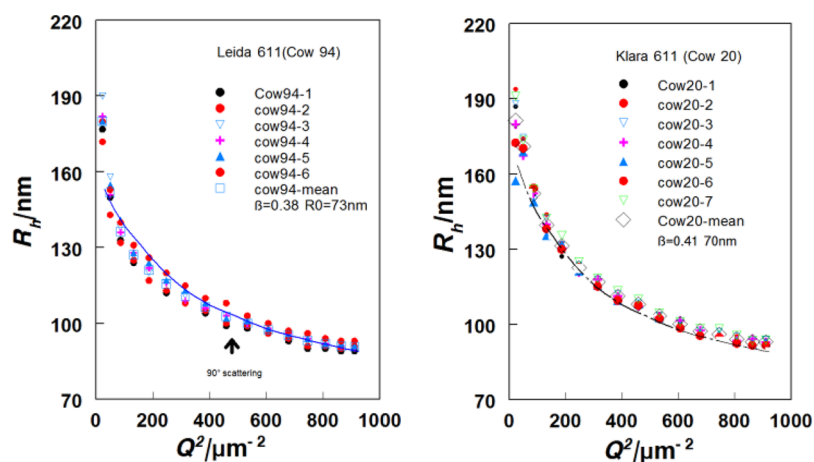


Figure 1. Hydrodynamic radius of casein micelles as a function of scattering wave vector squared for milk from two cows taken at several stages during a single evening milking. The drawn line is from simulation of an intensity autocorrelation function of a polydisperse sample. Polydispersity index and median radius are indicated.

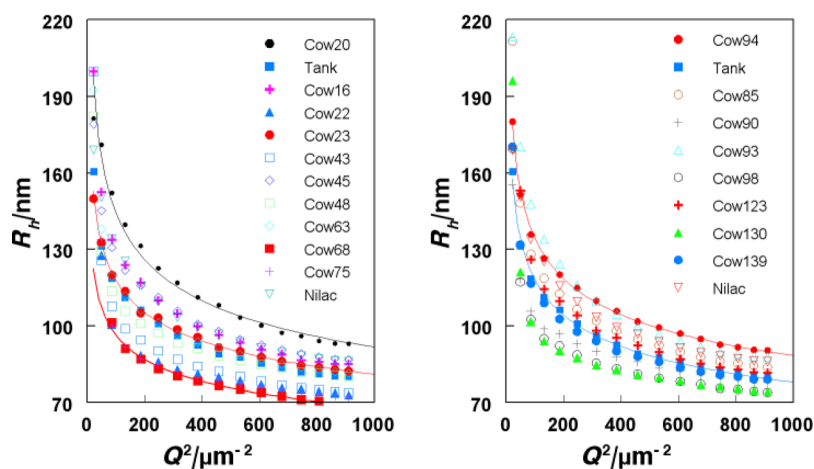


Figure 2. R_h as a function of Q^2 for milk samples from 18 different cows. Lines are a guide to the eye.

samples were taken in January 2006; milks from two cows were taken at six different time points during a single evening milking, so as to examine variability within one milking. In October 2007, a further sample was taken from one cow (cow 68). From March 2008, a further 16 cows were selected, from which milk samples were taken at 5 sampling points at approximate 4-week intervals. From one of these cows (cow 68), samples were also taken in two subsequent lactations, that is, in 2009 and 2010. Sodium azide (0.02%, m/m) and aprotinin (280 units mL⁻¹ milk) were added to all milk samples immediately after milking to prevent microbial growth and proteolysis by indigenous milk proteinases, respectively. Milk samples were defatted by centrifugation at 2000g for 30 min at 5 °C, followed by filtration through glass wool. Defatted samples were used for DLS measurements directly.

DLS measurements were made at 16 scattering angles, between 17 and 150°, on a multiangle ALV Compact Goniometer System (ALV-Laser Vertriebsgesellschaft m-bH, Langen, Germany) equipped with four detector units (ALV/GCS-4) and two ALV-5000/E multiple tau digital correlators. A Coherent Verdi V2 diode-pumped laser (Coherent, Inc., Santa Clara, CA, USA) was used, operating with vertically polarized light with a wavelength, λ , of 532.0 nm. Samples were diluted 100 times with milk serum prior to measurement (a previous investigation had highlighted that a minimum 50-fold dilution was required to avoid multiple scattering). All DLS data were analyzed using a second cumulant analysis. A third cumulant analysis showed that the data could be described adequately with a second cumulant fit. In DLS a relaxation spectrum is measured, which is translated into an

apparent hydrodynamic radius, R_h , using the Stokes–Einstein relationship

$$D = \frac{kT}{6\pi\eta R_h}$$

which relates the diffusion coefficient (D) to R_h of a particle, using the viscosity (η) of the milk serum, which was determined to be 1.032 mPa·s. It is not correct to use the viscosity of water because the continuous phase for the casein micelles is serum phase.

Sedimentation coefficient data were obtained at 1157g at 25 °C using an analytical centrifuge (LUM GmbH, Berlin, Germany), which measures the sedimentation velocity at low centrifugal force.

Viscosity measurements were made using an Ubbelohde viscometer in a water bath at 25.00 ± 0.01 °C.²³

Casein composition as determined by reversed-phase high-performance liquid chromatography (RP-HPLC).²⁴

RESULTS

Hydrodynamic Radius of Casein Micelles: Variation within One Milking. During the first sampling on January 30, 2006, milk was collected from two cows at six different time points during a single evening milking. Figure 1 shows R_h as a function of the scattering wave vector, Q (where $Q = 4\pi n \sin(\Theta/2)/\lambda$ and n is the refractive index of the dispersion medium, that is, milk serum ($n = 1.3410$), λ is the wavelength of the laser used ($\lambda = 532$ nm), and Θ is the scattering angle).

Figure 1 clearly shows that for the milk of both cows, R_h increases somewhat at low scattering angles, which indicates a degree of polydispersity in size distribution of the casein micelles and is discussed in further detail below. However, the main conclusion from Figure 1 is that casein micelle size does not vary during a single milking of a cow. The variation in hydrodynamic radius at 90° scattering is smaller than ± 3 nm and is a typical value for all measurements presented below.

The slight upswing at the smallest angles (Figure 1) is beyond doubt due to the presence of very small amounts of casein micelle aggregates or dust. The variation/noise at the smallest angles in contrast to the very constant values at higher angles is proof for this assumption. Our measurements indicate that values become reliable at $Q^2 > 250 \mu\text{m}^{-2}$, which corresponds to a scattering angle $>60^\circ$. Below that value, data become increasingly more noisy, despite careful defatting and the use of filtered milk serum for dilution. If a longer wavelength laser is used, the critical scattering angle will increase concomitantly.

Hydrodynamic Radius of Casein Micelles in Milk of Different Cows. During a 20-week period, we collected the milk of 16 cows and determined both casein micelle size and casein composition. Figure 2 shows R_h for the milk of the different cows as a function Q^2 and highlights clear differences between the milks of individual cows. In addition, Figure 3

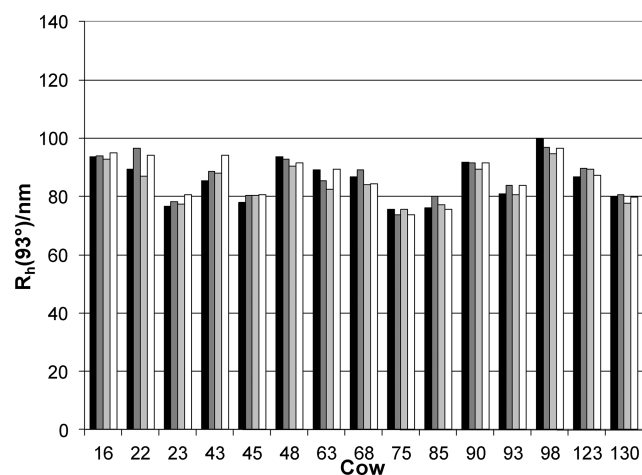


Figure 3. R_h at a scattering angle of 93° in the milk of 15 individual cows taken at 4 different time points during a single lactation.

shows R_h at one particular scattering angle, 93.5° for all cows as a function at different stages during lactation. The overriding conclusion from Figures 2 and 3 is that R_h varies between cows, but does not vary as a function of stage of lactation. One cow (cow 105) was even in its estrous cycle at one point of sampling, and even for this particular case, no variation in micelle size was detected.

To study the effect of different lactations on casein micelle size, the milk from cow 68 was selected; milk from this cow was collected in subsequent years. In total, eight milk samples from this cow were taken, one in 2007, five in 2008, one in 2009, and one in 2010. The measured values for R_h are presented in Figure 4 and show that casein micelle size remained constant, even over a 3-year period.

The fact that R_h did not change during milking (Figure 1), during lactation (Figures 2 and 3), or even over a period of 3 years (Figure 4) suggests that casein micelle size is strongly

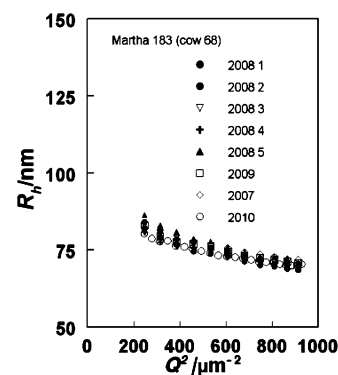


Figure 4. R_h for milk from cow 68 as a function of Q^2 . Samples were taken at one time point in 2007, 2009, and 2010 and at five different time points in 2008.

genetically determined and is extremely constant in the milks of individual cows. This constantness of casein micelle size of milk of individual cows contrasts with the results of Holt and co-workers,^{25–27} who determined variability of casein micelles size using turbidity and DLS. We believe this is due to the use of low scattering angles (40°) in those studies,^{25–27} where, as shown in Figures 1, 3, and 4, results are extremely sensitive to the presence of dust particles, residual clusters, or fat globules.

In Table 1 details are presented of the cows from which the milk was used in this study, as well as compositional parameters

Table 1. Details of Cows from Which Milk Was Used in This Study and Average Fat and Protein Contents of the Milks Used

cow	cow name	age (years)	lactations	fat (% m/m)	protein (% m/m)
16	Klara 657	4	3	4.77	3.60
22	Lien 376	2	1	4.04	3.53
23	Lien 374	2	1	4.52	3.42
43	Lien 295	8	6	3.99	3.23
45	Klara 561	5	3	4.86	3.73
48	Klara 580	9	8	4.69	3.80
63	Klara 629	6	4	4.92	3.72
68	Martha 183	6	4	4.91	3.48
75	Klara 675	3	2	4.63	3.44
85	Klara 696	2	1	4.96	3.63
90	Klara 660	4	3	4.95	3.49
93	Klara 555	10	9	4.99	3.43
98	Lien 275	10	9	4.73	3.47
123	Klara 623	6	5	3.66	3.27
130	Gerda 494	5	3	4.71	3.89
139	Lien 349	4	3	5.24	3.40

of the milk. By using R_h at scattering angles of 93° and 150° as representative values, we tried to correlate R_h to the values in Table 1. However, no correlations could be found between the parameters given in Table 1 and R_h .

Polydispersity in Casein Micelle Hydrodynamic Radius. One aspect that draws attention from Figures 1, 2, and 4 is that the upswing at small Q increases when R_h increases, indicating a correlation between R_h and polydispersity. Therefore, the polydispersity of casein micelle size distributions was analyzed in further detail. For a truly monodisperse system, R_h does not vary as a function of scattering angle, but for a polydisperse system, apparent R_h

increases toward small scattering angles, because the measurement is a weighted average, that is, $R_h \sim [R^6]/[R^5]$. In principle, mean particle size and polydispersity can be extracted from the intensity autocorrelation function. In practice, however, this is not straightforward, because the problem is a so-called ill-posed problem; that is, deconvolution of the correlation function is ambiguous. Upon the addition of some noise to noise-free computer-generated correlation functions, several solutions fit the generated data set equally well. The obtained values for mean particle size and polydispersity depend on the regularization strength in the algorithm used.²⁸ Especially if some noise is present, data can be fitted equally well with a three-parameter cumulant or a four-parameter double-exponential. What can be done unambiguously, however, is the following: sedimentation field flow fractionation experiments showed that the size distribution of casein micelles closely resembles a log-normal distribution,²⁹ which is given by

$$f_{\ln}(r) = \frac{1}{(r\beta\sqrt{2\pi})} \exp \left[- \left(\frac{\ln\left(\frac{r}{R_{10}}\right)}{\beta\sqrt{2}} \right)^2 \right]$$

where β is a measure for relative polydispersity and is related to σ , the relative standard deviation in a Gaussian distribution, by

$$\beta \approx \sqrt{\ln(\sigma_{\text{std}}^2 + 1)}$$

For not too large values, $\beta \approx \sigma$. R_{10} is the mean particle radius, also called the modal value.

Assuming a particle size and a polydispersity, it is straightforward to calculate an intensity autocorrelation function, $g_2(t, \Theta)$, as is measured in DLS. We simulated $g_2(t, \Theta)$, using exactly the same time scale as is used in the hardware of the correlator, and fitted the simulated data to the same second cumulant fit as the experimental data. It appeared that even simulating $g_2(t, \Theta)$ with a different, for example, linear, time axis and then fitting the noise-free data already gives a different result. The adjustable variables in this simulation are R_{10} and β . In case the casein micelles would have an inhomogeneous scattering length distribution, that parameter must be included as well. However, neutron scattering contrast variation shows that the radius of gyration is independent of scattering contrast.¹⁷ On the basis of electron microscopy it is assumed that the particles are spheroids.^{7,8}

Figure 5 shows a typical result obtained from the procedure outlined above for estimating polydispersity, with the drawn lines representing the simulated, and subsequently second cumulant-fitted, data. All calculated R_h values were obtained from the calculated D , using the aforementioned Stokes–Einstein equation. It must be noted that it is the Q dependence of the particle scattering that causes the apparent particle radius to vary. The drawn curves are unique in the sense that there is only one combination of R_{10} and β possible. If the scattering properties are changed, other combinations become possible, but, then, a third parameter is introduced. The results in Figures 2 and 5 can be summarized as follows: from the cows investigated, the milk of cow 68 had the smallest casein micelles, corresponding to an $R_{10} = 55$ nm and a polydispersity $\beta = 0.27$. The experimentally found R_h at $\Theta = 150^\circ$ scattering is 63 nm. It is noted that the experimental R_g is smaller than would follow from the given modal size and polydispersity, which probably indicates that the micelles are even more

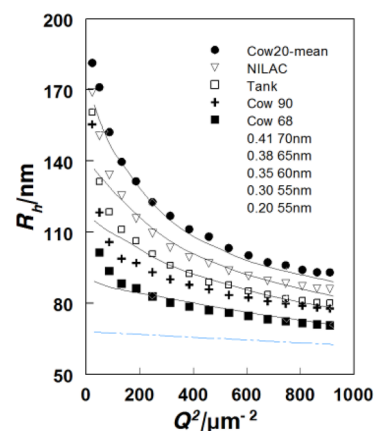


Figure 5. Experimental R_h versus Q^2 for several representative samples. The drawn lines were from simulated data. Size and polydispersity decrease from top to bottom as indicated in the legend.

monodisperse than assumed. For the milk of cow 20 (the most polydisperse), $R_h(\Theta = 150) = 89$ nm, $R_{10} = 70$ nm and $\beta = 0.41$. It is remarkable that all other values are between these two extremes. Bulk milk from the herd from which the samples were taken is just between, that is, $R_{10} = 60$ nm, $\beta = 0.35$, and $R_h(\Theta = 150) = 78$ nm. These data thus indicate that size and polydispersity are related. Figure 6 shows a plot of estimated

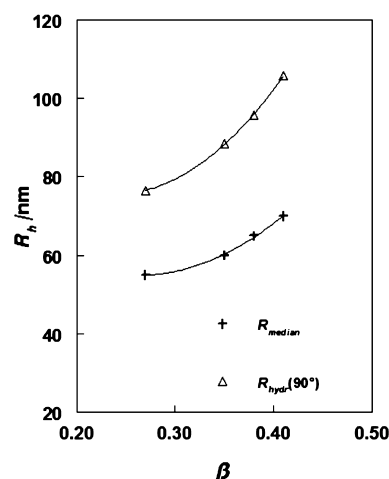


Figure 6. Hydrodynamic radius versus polydispersity (β). The drawn lines are quadratic functions of β .

polydispersity from the simulations and the modal casein micelle radius and the experimental DLS radius, which is a $\langle R^6 \rangle / \langle R^5 \rangle$ average, at two scattering angles, $R_h(\Theta = 150)$ and $R_h(\Theta = 90)$. From the data it appears that micelle radius scales on polydispersity (quadratic). Such a relationship is also encountered for surfactant microemulsions.^{30,31}

Casein Composition of the Casein Micelles. Casein composition was determined by RP-HPLC of the milk of 15 different cows at 4 stages of lactation. The four caseins, α_{s1} -casein, α_{s2} -casein, β -casein, and κ -casein, were quantified, and the results shown in Figure 7 clearly highlight that only small differences in casein composition were observed between cows and that casein composition was extremely constant for each cow as a function of stage of lactation. In all samples analyzed, α_{s1} -casein, α_{s2} -casein, β -casein, and κ -casein represented ≈ 37 , ≈ 8 , ≈ 45 , and $\approx 10\%$ of total casein peak area.

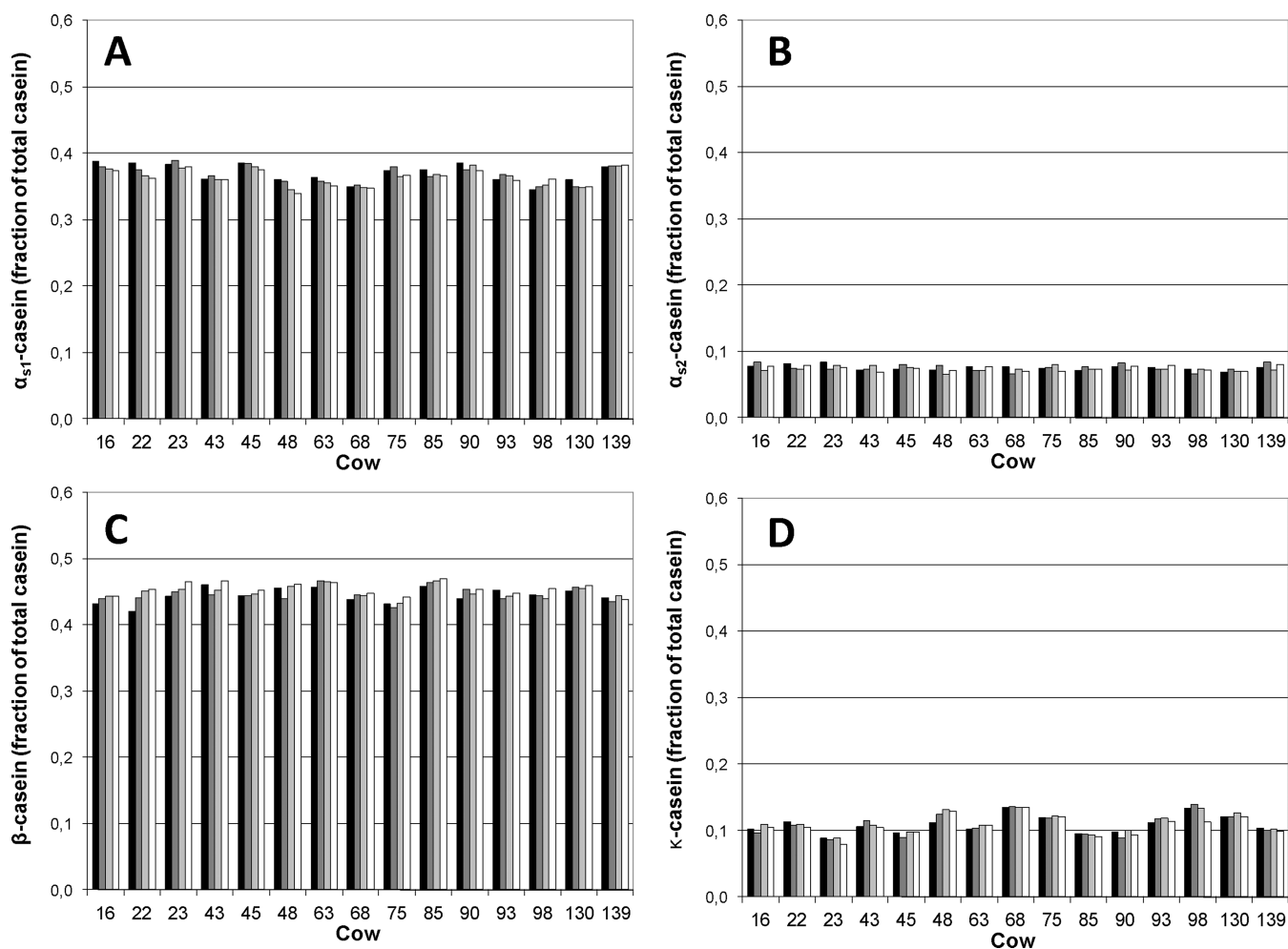


Figure 7. Proportion of (A) α_{s1} -casein, (B) α_{s2} -casein, (C) β -casein, and (D) κ -casein as a function of total casein peak area in the milk of 15 individual cows taken at 4 different time points during lactation.

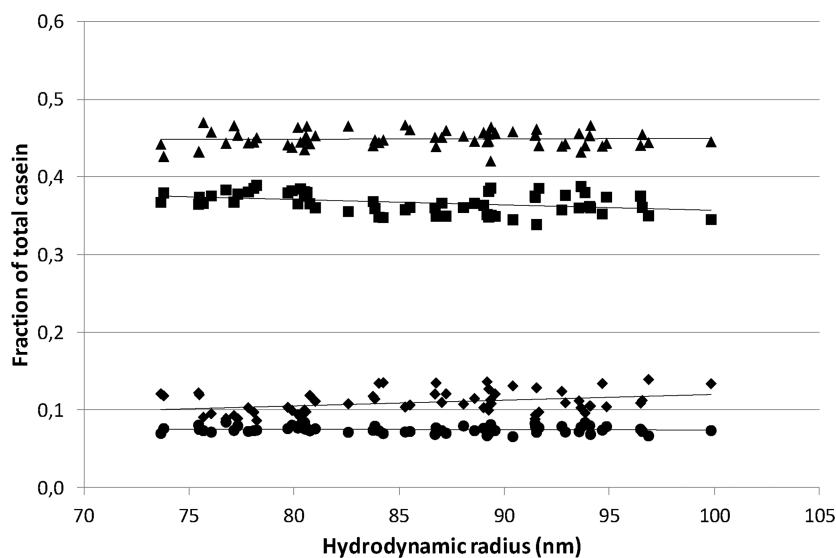


Figure 8. Proportion of α_{s1} -casein (■), α_{s2} -casein (●), β -casein (▲), and κ -casein (◆) of total casein peak area in milk from individual cows expressed as a function of hydrodynamic radius.

Figure 8 shows the relative proportion of each of the caseins as a function of R_h and shows that average casein micelle size does not affect casein composition, or vice versa. For all caseins,

no significant correlation could be found between the proportion of the respective casein in milk and R_h values; for α_{s1} -casein, α_{s2} -casein, β -casein, and κ -casein, R^2 values were

found to be 0.14, 0.02, 0.00, and 0.11, respectively. These results contrast with previous reports^{32–37} that κ -casein content decreases with increasing micelle size. It should be noted, however, that such reports derive primarily from size classes of casein micelles from the centrifugal fractionation of bulk milk, whereas we correlated micelle size to casein composition in the milk of individual cows.

Devold et al.³⁸ reported on the size and protein composition, including genetic variation, of the casein micelles in the milk of a herd of 58 Norwegian short horns. DLS data were obtained at 90° only and using a laser with a wavelength of 633 nm, corresponding to $Q^2 = 350 \mu\text{m}^{-2}$, which is equivalent to a scattering angle of 73° in the setup of the present investigation. The variation found in particle radius for the Norwegian short horns, that is, from 75 to 111 nm,³⁸ is nearly identical to the spread in the size of casein micelles in the milk of the Holstein-Friesians (Figures 2 and 3). On the basis of our own data, the experimental uncertainty at $Q^2 = 350 \mu\text{m}^{-2}$ is estimated to be ≈ 4 nm. Casein micelle size in the milk of the Norwegian short horns was found to be correlated with feeding regime and genetic variety of the proteins.³⁸ These findings could not be confirmed in the current study, even though milk samples were collected in periods when the cows were both corn plus silage fed (winter) and grass fed (spring/summer).

Voluminosity. The voluminosity (q) of casein micelles is needed to determine their volume fraction, ϕ , that is, $\phi = q \times c$, where c is the weight concentration. We prefer to use the hydrodynamic volume, as found from dilute viscosity measurements, because sediment volumes depend on occluded volumes, particle interactions, and centrifugal forces. Using the Einstein viscosity equation to measure voluminosity²³ of casein micelles in the milk of cow 68, we found $q = 4.4 \text{ mL/g}$ (data not shown), in agreement with previous results.^{19,23}

Density of Casein Micelles. Sedimentation velocity $U(R)$ of casein micelles was determined by detecting the sedimenting particle front during analytical centrifugation. For tank milk, diluted with milk permeate, six samples, differing in casein micelle volume fraction, were measured and used for the determination of the sedimentation coefficient, S , which is defined as

$$S(R) = \frac{U(R)}{\omega^2 r}$$

in which R is particle radius, r the distance of the particles to the center of rotation, and ω the angular velocity, which is equivalent to 2000 rpm. Figure 9 shows the experimental sedimentation velocity as a function of the volume fraction of casein micelles.

The experimental data extrapolate back to $U_0 = 2.67 \mu\text{m/s}$. We used a centrifugal acceleration of 1157g, which results in 2380 Svedberg seconds. The slope of the normalized function $U/U_0 = -4.9$. For hard spheres the slope is calculated by Batchelor³⁹ as -6.55 . We used the S_0 value for determining casein micelle density, which also requires a particle radius. The instrument weighs the data by M^2 , as it uses light transmission to detect the sedimenting particle front. The radius found by this method is just like a radius of gyration, that is, an $\langle R^8 \rangle / \langle R^6 \rangle$ average. For the tank milk samples used, we found $R_{10} = 60 \text{ nm}$ and $\beta = 0.35$. Using these values it is calculated that the density difference of the casein micelles is $\Delta\rho_{\text{CM}} = 0.055 \text{ kg/L}$. Because the density of the serum was $\rho_{\text{serum}} = 1.023 \text{ kg/L}$, the casein micelles have a density $\rho_{\text{CM}} = 1.078 \text{ kg/L}$. The interior of a casein micelle can be viewed as a concentrated polymer

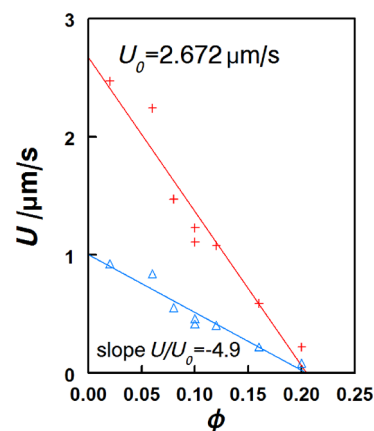


Figure 9. Sedimentation velocity, U , of casein micelles at 1157g as a function of volume fraction.

solution, so it is assumed that the casein micelles sediment as solid, nondraining, nanogel particles, because internal friction will be very high. On the basis of the hydrodynamic voluminosity, we calculate the density of the micellar solids, that is, casein plus MCP, from

$$\rho_{\text{CM}} = 1/4.4\rho_{\text{Cas}} + 3.4/4.4\rho_{\text{serum}}$$

which results in

$$\rho_{\text{Cas}} = 1.42 \text{ kg/L}$$

Morris et al.¹⁹ measured hydrodynamic properties of casein micelles and, from viscosity measurements, reported a voluminosity of 4.2 mL/g, in accordance with the value found herewith (4.4 mL/g). They report a value for the diffusion coefficient that translated into a hydrodynamic radius of 78.8 nm, again consistent with values reported here. The sedimentation coefficient, however, was reported as 845 S,¹⁹ whereas we find 2380 S (Figure 9). This considerable difference can be attributed to the considerably higher angular velocity (12600 rpm) applied by Morris et al.,¹⁹ which can present difficulties in the measurement of casein micelles due to their fast sedimentation. Morris et al.¹⁹ give a concentration dependence of the sedimentation coefficient (using their 4.2 mL/g) of -4 , which is slightly lower, but still in agreement with, the slope of -4.9 found in the present study (Figure 9).

Morris et al.¹⁹ report a molecular mass of $2.8 \times 10^8 \text{ Da}$, whereas we find a value of $7.6 \times 10^9 \text{ Da}$, a factor of 27 larger. The value of Morris et al.¹⁹ depends very much on the assumed particle radius, particularly on which moment of the size distribution is used. In sedimentation experiments using light scattering, a $\langle R^8 \rangle / \langle R^6 \rangle$ average is measured. For tank milk, this was 141 nm. Inserting this value leads to a lower particle density (1043 kg m^{-3}), but calculating the molar mass leads to a value of $7.4 \times 10^9 \text{ Da}$, virtually the same value as ours. This illustrates that in calculating a property of a polydisperse system, it is required to use the correct particle average. At a constant weight fraction and volume fraction, it follows that $N_{\text{CM}} \times 4/3\pi R^3 = \text{constant}$. The question arises which value to use for R ? The volume fraction is constant and follows from the Einstein viscosity, and therefore it is a volume average. The volume-average radius for pooled milk is 71 nm. Using this value gives a value for molecular mass that is almost 10 times smaller, using the same density as above. Therefore, the use of different weight averages leads to an apparent discrepancy between data reported in the literature, so actually one must

use the (weighted) integral over the particle size distribution rather than taking a (weighted) average particle size.

The results presented herewith show that, in contrast to literature reports, individual cows produce quite monodisperse casein micelles. The size distribution of the micelles is extremely constant, that is, it does not change within one milking, within a lactation, or even over consecutive lactations. The modal radii vary from 55 to 70 nm, the hydrodynamic radius at 73° scattering varies between 77 and 115 nm, and polydispersity varies from 0.27 to 0.41. The variation in size and concomitant polydispersity cannot be attributed to the κ -casein content of the micelles, because casein composition did not vary either as a function of the aforementioned parameters. In addition, no correlations between particle size and casein composition were observed. However, there is no clear indication why there is a variation in size.

AUTHOR INFORMATION

Corresponding Author

*Email: DeKruif@NIZO.NL.

Notes

The authors declare no competing financial interest.

ACKNOWLEDGMENTS

We thank Mary Smiddy, Jan Klok, and Charles Slangen (NIZO food research) for skillful technical assistance and Henk de Kruif and my (C.G.K.) nephew Kees de Kruif for providing the milk samples from their herd of Holstein-Friesians.

REFERENCES

- (1) Lucey, J. A.; Horne, D. S. In *Advanced Dairy Chemistry 3 – Lactose, Water Salts and Minor Constituents*, 3rd ed.; McSweeney, P. L. H., Fox, P. F., Eds.; Springer: New York, 2009; p 351.
- (2) Holt, C. *J. Dairy Res.* **1982**, *49*, 29–38.
- (3) Chaplin, L. C. *J. Dairy Res.* **1984**, *51*, 251–257.
- (4) Neville, M. C. *J. Mammary Gland Biol. Neoplasia* **2005**, *10*, 119–128.
- (5) Fox, P. F. In *Advanced Dairy Chemistry 1 – Proteins*, 3rd ed.; Fox, P. F., McSweeney, P. L. H., Eds.; Kluwer Academic/Plenum Publishers: New York, 2003; p 1.
- (6) Swaisgood, H. E. In *Advanced Dairy Chemistry 1 – Proteins*, 3rd ed.; Fox, P. F., McSweeney, P. L. H., Eds.; Kluwer Academic/Plenum Publishers: New York, 2003; p 139.
- (7) Schmidt, D. G. In *Developments in Dairy Chemistry*; Fox, P. F., Ed.; Applied Science Publishers: Barking, U.K., 1982; p 61.
- (8) Rollema, H. S. In *Advanced Dairy Chemistry 1 – Proteins*, 2nd ed.; Fox, P. F., Ed.; Elsevier Applied Science: Barking, U.K., 1992; p 111.
- (9) Holt, C. *Adv. Protein Chem.* **1992**, *43*, 63–151.
- (10) Holt, C.; Horne, D. S. *Neth. Milk Dairy J.* **1996**, *50*, 1–27.
- (11) De Kruif, C. G. In *Progress in Biotechnology: Industrial Proteins in Perspective*; Aalbersberg, W. Y., Hamer, R. J., Jasperse, P., de Jongh, H. H. J., de Kruif, C. G., Walstra, P., de Wolf, F. A., Eds.; Elsevier Science: Amsterdam, The Netherlands, 2003; p 259.
- (12) De Kruif, C. G.; Holt, C. In *Advanced Dairy Chemistry 1 – Proteins*, 3rd ed.; Fox, P. F., McSweeney, P. L. H., Eds.; Kluwer Academic/Plenum Publishers: New York, 2003; p 233.
- (13) Fox, P. F.; Brodtkorb, A. *Int. Dairy J.* **2008**, *18*, 695–704.
- (14) Horne, D. S. *Curr. Opin. Colloid Interface Sci.* **2002**, *7*, 456–461.
- (15) Horne, D. S. *Curr. Opin. Colloid Interface Sci.* **2006**, *11*, 148–153.
- (16) Farrell, H. M., Jr.; Malin, E. L.; Brown, E. M.; Qi, P. X. *Curr. Opin. Colloid Interface Sci.* **2006**, *11*, 135–147.
- (17) De Kruif, C. G.; Huppertz, T.; Pethukov, A.; Urban, V. *Adv. Colloid Interface Sci.* **2012**, *171–172*, 36–52.
- (18) Dalgleish, D. G. *Soft Matter* **2011**, *7*, 2265–2272.
- (19) Morris, G. A.; Foster, T. J.; Harding, S. E. *Biomacromolecules* **2000**, *1*, 764–767.
- (20) Smyth, E.; Clegg, R.; Holt, C. *Int. J. Dairy Technol.* **2004**, *57*, 121–126.
- (21) Little, E. M.; Holt, C. *Eur. Biophys. J.* **2004**, *33*, 435–447.
- (22) De Kruif, C. G.; Zhulina, E. B. *Colloids Surf. A* **1996**, *117*, 151–159.
- (23) Jeurnink, T. J. M.; de Kruif, C. G. *J. Dairy Res.* **1993**, *60*, 139–150.
- (24) Visser, S.; Slangen, K. J.; Rollema, H. S. *J. Chromatogr., A* **1991**, *548*, 361–370.
- (25) Holt, C.; Parker, T. G.; Dalgleish, D. G. *Biochim. Biophys. Acta* **1975**, *400*, 283–292.
- (26) Holt, C.; Baird, L. *J. Dairy Res.* **1978**, *45*, 339–345.
- (27) Holt, C.; Muir, D. D. *J. Dairy Res.* **1978**, *45*, 347–353.
- (28) Kuipers, B. Personal communication, 2011.
- (29) De Kruif, C. G. *J. Dairy Sci.* **1998**, *81*, 3019–3028.
- (30) Overbeek, J. T. G. *Prog. Colloid Polym. Sci.* **1990**, *83*, 1–9.
- (31) Borkovec, M.; Eicke, H. F.; Ricka, J. *J. Colloid Interface Sci.* **1989**, *131*, 366–381.
- (32) Ekstrand, B.; Larsson-Raznikiewicz, M. *Biochim. Biophys. Acta* **1978**, *536*, 1–9.
- (33) McGann, T. C. A.; Donnelly, W. J.; Kearney, R. D.; Buchheim, W. *Biochim. Biophys. Acta* **1980**, *630*, 261–270.
- (34) Davies, T.; Law, A. J. R. *J. Dairy Res.* **1983**, *50*, 67–75.
- (35) Donnelly, W. J.; McNeill, G. P.; Buchheim, W.; McGann, T. C. A. *Biochim. Biophys. Acta* **1984**, *789*, 136–143.
- (36) Dalgleish, D. G. *Biochim. Biophys. Acta* **1985**, *830*, 213–215.
- (37) Dalgleish, D. G.; Horne, D. S.; Law, A. J. R. *Biochim. Biophys. Acta* **1989**, *991*, 383–387.
- (38) Devold, T. G.; Brovold, M. J.; Langsrud, T.; Vegarud, G. E. *Int. Dairy J.* **2000**, *10*, 313–323.
- (39) Batchelor, G. K.; Wen, C. S. *J. Fluid Mech.* **1982**, *124*, 495–528.